

# Distinct roles of matrix metalloproteases in the early- and late-phase development of neuropathic pain

Yasuhiko Kawasaki<sup>1,4</sup>, Zhen-Zhong Xu<sup>1,4</sup>, Xiaoying Wang<sup>2,4</sup>, Jong Yeon Park<sup>1</sup>, Zhi-Ye Zhuang<sup>1</sup>, Ping-Heng Tan<sup>1</sup>, Yong-Jing Gao<sup>1</sup>, Kristine Roy<sup>3</sup>, Gabriel Corfas<sup>3</sup>, Eng H Lo<sup>2</sup> & Ru-Rong Ji<sup>1</sup>

**Treatment of neuropathic pain, triggered by multiple insults to the nervous system, is a clinical challenge because the underlying mechanisms of neuropathic pain development remain poorly understood<sup>1–4</sup>. Most treatments do not differentiate between different phases of neuropathic pain pathophysiology and simply focus on blocking neurotransmission, producing transient pain relief. Here, we report that early- and late-phase neuropathic pain development in rats and mice after nerve injury require different matrix metalloproteinases (MMPs). After spinal nerve ligation, MMP-9 shows a rapid and transient upregulation in injured dorsal root ganglion (DRG) primary sensory neurons consistent with an early phase of neuropathic pain, whereas MMP-2 shows a delayed response in DRG satellite cells and spinal astrocytes consistent with a late phase of neuropathic pain. Local inhibition of MMP-9 by an intrathecal route inhibits the early phase of neuropathic pain, whereas inhibition of MMP-2 suppresses the late phase of neuropathic pain. Further, intrathecal administration of MMP-9 or MMP-2 is sufficient to produce neuropathic pain symptoms. After nerve injury, MMP-9 induces neuropathic pain through interleukin-1 $\beta$  cleavage and microglial activation at early times, whereas MMP-2 maintains neuropathic pain through interleukin-1 $\beta$  cleavage and astrocyte activation at later times. Inhibition of MMP may provide a novel therapeutic approach for the treatment of neuropathic pain at different phases.**

MMPs are widely implicated in inflammation and tissue remodeling associated with various neurodegenerative diseases through the cleavage of extracellular matrix proteins, cytokines, and chemokines<sup>5–10</sup>. We hypothesized that neuropathic pain and neuroinflammation may share similar mechanisms. Therefore, we set out to study the roles of the two main gelatinases, MMP-2 and MMP-9, in the pathophysiology of neuropathic pain using a well characterized animal model, L5 spinal nerve ligation (SNL)<sup>11</sup>.

Because nerve injury-induced changes in the DRG are essential for the generation of neuropathic pain<sup>1</sup>, we examined gelatinase activity

in injured (L5) DRGs. Gelatin zymography showed very low activity of MMP-9 in the naive DRG (Fig. 1a). SNL induced rapid but transient upregulation of MMP-9 activity, peaking within the first day and declining after 3 d. In contrast, MMP-2 activity showed delayed upregulation, occurring on day 7 and still present on day 21 (Fig. 1a). SNL also increased MMP-9 expression on day 1 but not day 10 (Fig. 1b). The active form of MMP-9 was weak and not well separated from pro-MMP-9 (Fig. 1a,b, Supplementary Fig. 1a,b online). MMP-9 was expressed in DRG neurons, and more MMP-9<sup>+</sup> neurons were found after SNL (Fig. 1c). In cultured DRG neurons, tumor necrosis factor- $\alpha$  (TNF- $\alpha$ ) and interleukin-1 $\beta$  (IL-1 $\beta$ ), the proinflammatory cytokines that are rapidly produced after tissue injury, increased both the expression and release of MMP-9 (Supplementary Fig. 1c,d). A TNF- $\alpha$  inhibitor further suppressed SNL-induced MMP-9 upregulation (Supplementary Fig. 1e). Notably, neuronal activity was sufficient to release MMP-9 from DRG neurons (Supplementary Fig. 1f). In the spinal cord dorsal horn where secondary nociceptive neurons are localized, MMP-9 activity was very low, and SNL only moderately increased MMP-9 expression (Supplementary Fig. 1g). MMP-9 in the spinal cord originated partly from dorsal root axonal transport from DRG neurons, because MMP-9 in the dorsal horn was colocalized with calcitonin gene-related peptide, a peptide that is expressed in nociceptive primary afferents (Supplementary Fig. 1h).

Neuropathic pain is characterized by mechanical allodynia—that is, painful responses to previously non-painful mechanical stimuli. To define the role of MMPs in neuropathic pain development, we used five different approaches: (i) small synthetic inhibitors, (ii) endogenous peptide inhibitors, (iii) small interfering RNAs, (iv) exogenous MMP injection and (v) knockout mice. To avoid systemic effects of drugs, we delivered them into spinal fluid by intrathecal (i.t.) administration, with the goal of targeting MMP in the DRG and spinal cord<sup>12</sup>.

First, we continuously infused a small synthetic anthranilic acid-based MMP-9 inhibitor<sup>13</sup> for 1 week with an osmotic pump. This treatment delayed the development of mechanical allodynia for 11 d (Fig. 2a). Bolus injections of the inhibitor for 5 d produced a gradually

<sup>1</sup>Pain Research Center, Department of Anesthesiology, Brigham and Women's Hospital and Harvard Medical School, 75 Francis Street, Medical Research Building, Room 604, Boston, Massachusetts 02115, USA. <sup>2</sup>Neuroprotection Research Laboratory, Departments of Neurology and Radiology, Massachusetts General Hospital and Harvard Medical School, 149 13<sup>th</sup> Street, Charlestown, Massachusetts 02129, USA. <sup>3</sup>Division of Neuroscience, Children's Hospital and Harvard Medical School, 300 Longwood Avenue, Boston, Massachusetts 02115, USA. <sup>4</sup>These authors contributed equally to this study. Correspondence should be addressed to R.-R.J. (rrji@zeus.bwh.harvard.edu).

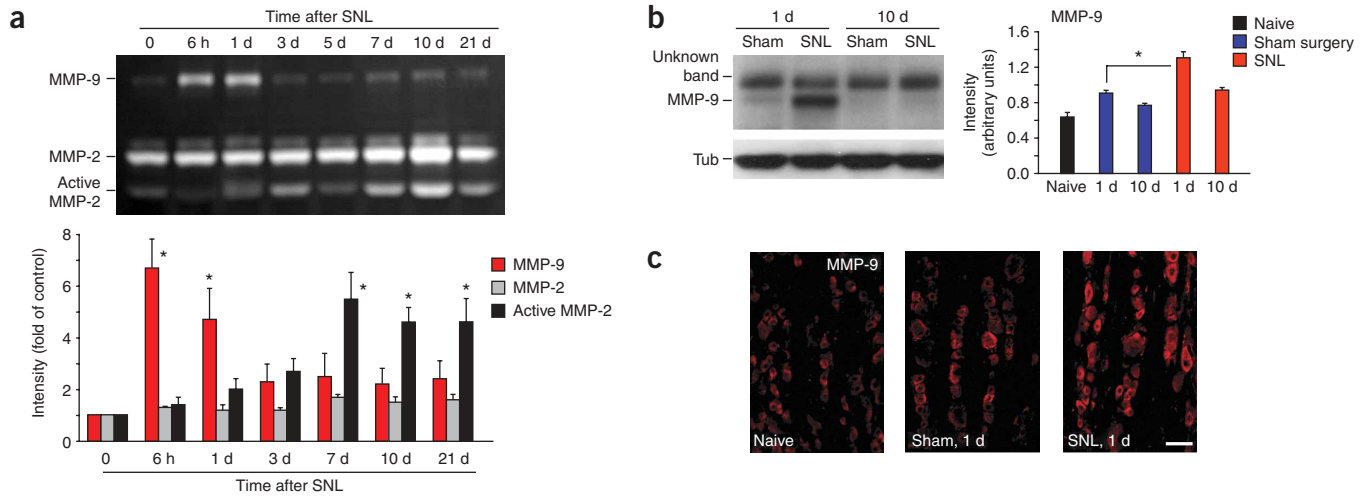


**Figure 1** Upregulation of MMP-9 in the DRG after SNL. **(a)** Gelatin zymography showing the time course of MMP-9 and MMP-2 activity in the injured L5 DRG of SNL rats. Bottom, intensity of specific MMP bands, expressed as multiples of the values in uninjured control ( $*P < 0.05$  compared to control,  $n = 5$ ). **(b)** MMP-9 western blot of the L5 DRGs of sham and SNL rats. Right, quantification of MMP-9 band intensity ( $*P < 0.05$ ,  $n = 3$ ). Tub,  $\beta$ -tubulin. **(c)** MMP-9 immunohistochemistry in the L5 DRG of control and SNL rats. MMP-9 is expressed in DRG neurons. Scale bar, 50  $\mu$ m. All data are mean  $\pm$  s.e.m.

decreasing antiallodynic effect over time (**Supplementary Fig. 2a** online). Recombinant TIMP-1, an endogenous tissue inhibitor of MMP-9 (ref. 14), when given 1 d after SNL, was highly effective in attenuating allodynia. A single injection (4 pmol) reversed allodynia for more than 24 h in the early phase (**Fig. 2b**). However, TIMP-1 had no effect on allodynia when given 10 d after nerve injury (**Supplementary Fig. 2b**). In support of the results with MMP-9 inhibitors, small interfering RNA (siRNA,  $2 \times 5 \mu$ g, i.t.) targeted against *Mmp9*

*in vivo* successfully suppressed DRG MMP-9 activity and expression after SNL and delayed the development of allodynia (**Fig. 2c**, **Supplementary Fig. 3a–c** online). Conversely, a single injection of exogenous MMP-9 (1 pmol, i.t.) produced rapid mechanical allodynia, which faded at 6 d (**Fig. 2d**).

To further confirm our pharmacological data, we assessed neuropathic pain in mice lacking MMP-9 (*Mmp9*<sup>-/-</sup>). SNL induced robust spontaneous pain in wild-type FVB mice, especially in the

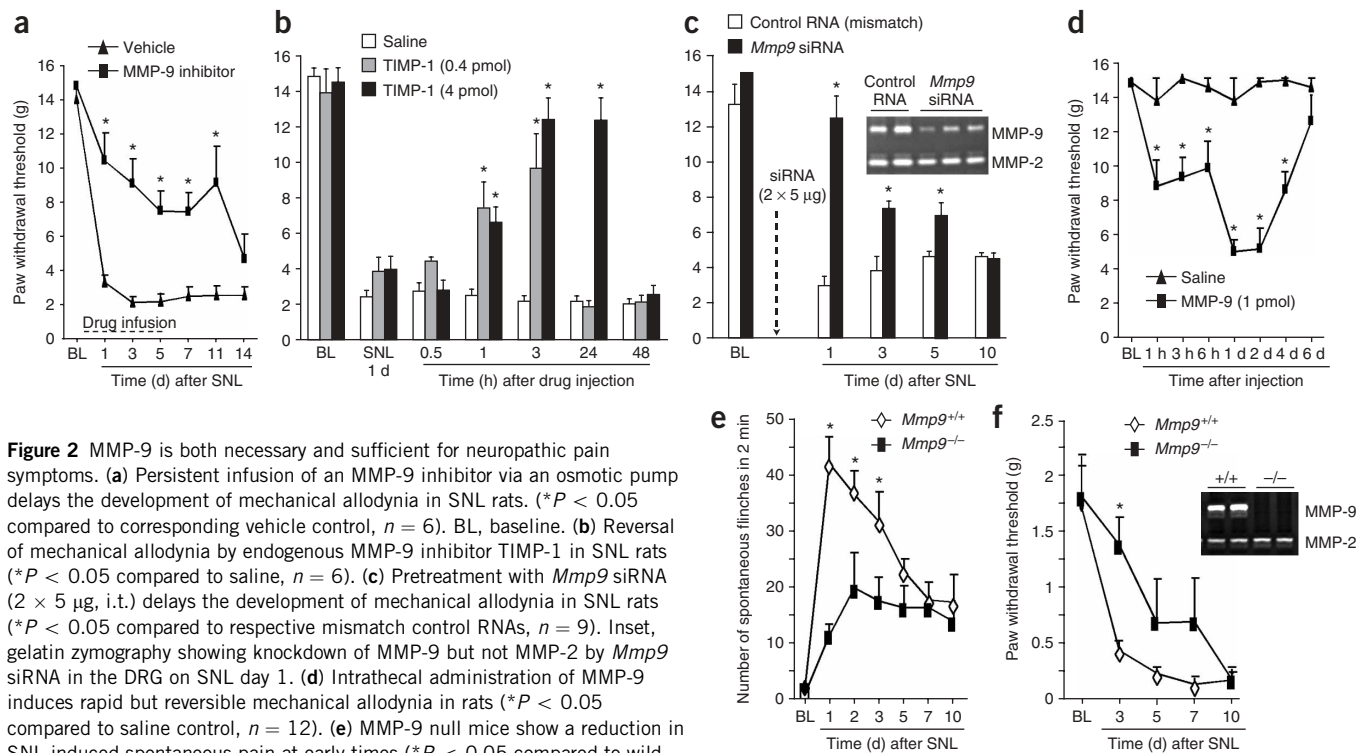


**Figure 2** MMP-9 is both necessary and sufficient for neuropathic pain symptoms. **(a)** Persistent infusion of an MMP-9 inhibitor via an osmotic pump delays the development of mechanical allodynia in SNL rats. ( $*P < 0.05$  compared to corresponding vehicle control,  $n = 6$ ). BL, baseline. **(b)** Reversal of mechanical allodynia by endogenous MMP-9 inhibitor TIMP-1 in SNL rats ( $*P < 0.05$  compared to saline,  $n = 6$ ). **(c)** Pretreatment with *Mmp9* siRNA ( $2 \times 5 \mu$ g, i.t.) delays the development of mechanical allodynia in SNL rats ( $*P < 0.05$  compared to respective mismatch control RNAs,  $n = 9$ ). Inset, gelatin zymography showing knockdown of MMP-9 but not MMP-2 by *Mmp9* siRNA in the DRG on SNL day 1. **(d)** Intrathecal administration of MMP-9 induces rapid but reversible mechanical allodynia in rats ( $*P < 0.05$  compared to saline control,  $n = 12$ ). **(e)** MMP-9 null mice show a reduction in SNL-induced spontaneous pain at early times ( $*P < 0.05$  compared to wild-type mice,  $n = 6$ ). **(f)** MMP-9 null mice show a reduction of mechanical allodynia at early times after SNL ( $*P < 0.05$  compared to wild-type mice,  $n = 6$ ). Inset, gelatin zymography showing absence of MMP-9 in MMP-9 null mice. All data are mean  $\pm$  s.e.m.

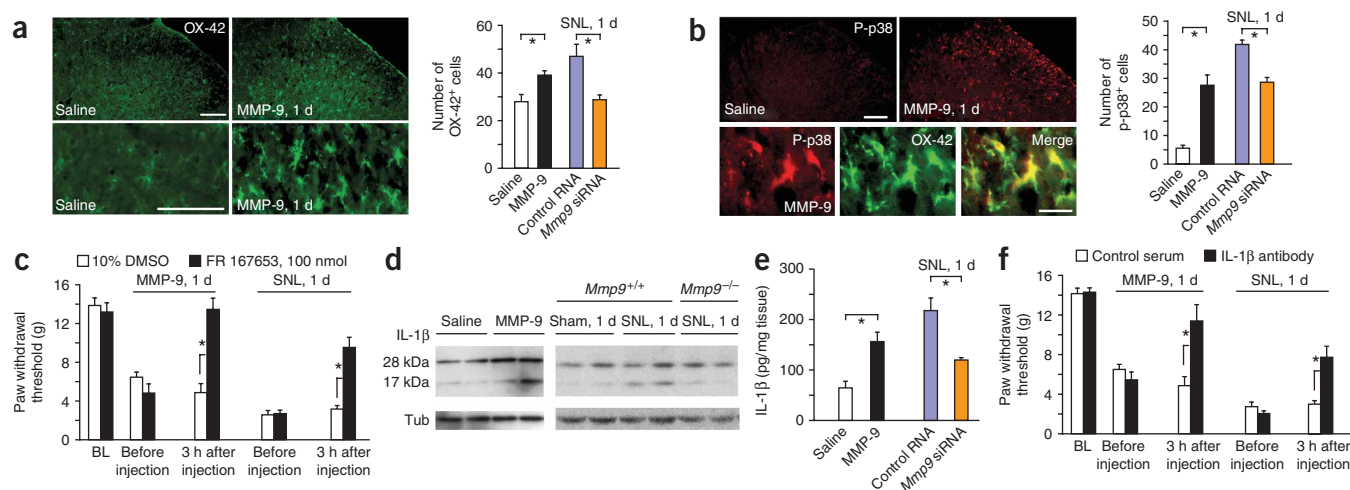


**Figure 3** MMP-9 produces neuropathic pain through microglial activation and IL-1 $\beta$  signaling.

(a) Immunostaining for OX-42 in rat dorsal horn after intrathecal saline or MMP-9 (1 pmol). Bottom, high magnification of microglia. Scale bars, 50  $\mu$ m. Right, number of OX-42<sup>+</sup> microglia after treatment with MMP-9 and *Mmp9* siRNA (2  $\times$  5  $\mu$ g) in rats ( $*P < 0.05$ ,  $n = 4$ ). (b) Immunostaining for phospho-p38 (P-p38) in the dorsal horn after intrathecal MMP-9 (1 pmol). Bottom, colocalization of P-p38 and OX-42 in spinal microglia after MMP-9 treatment. Scale bars, 50  $\mu$ m (top) and 10  $\mu$ m (bottom). Right, number of P-p38<sup>+</sup> cells in the dorsal horn after treatment with MMP-9 and *Mmp9* siRNA ( $*P < 0.01$ ,  $n = 4$ ). (c) p38 inhibitor FR167653 (100 nmol, i.t.) blocks mechanical allodynia induced either by MMP-9 (1 pmol) or SNL ( $*P < 0.05$ ,  $n = 6$ ). (d) Left, intrathecal MMP-9 (1 pmol) induces IL-1 $\beta$  cleavage in the DRG. Right, IL-1 $\beta$  cleavage after SNL is reduced in MMP-9 null mice. (e) ELISA showing DRG IL-1 $\beta$  concentrations after treatment with MMP-9, SNL and *Mmp9* siRNA ( $*P < 0.05$ ,  $n = 4-6$ ). Tub,  $\beta$ -tubulin. (f) IL-1 $\beta$ -neutralizing antibody (5  $\mu$ g, i.t.) reverses mechanical allodynia induced by MMP-9 and SNL ( $*P < 0.05$ ,  $n = 6$ ). (g) Schematic of MMP-9-triggered events in the genesis of neuropathic pain. MMP-9 upregulation after nerve injury increases IL-1 $\beta$  cleavage in the DRG and spinal cord. MMP-9 and IL-1 $\beta$  are transported to spinal central terminals. Dashed arrows, previously known events. A positive feedback loop between IL-1 $\beta$  and p38 can enhance the production of IL-1 $\beta$ , leading to increased pain sensitivity. All data are mean  $\pm$  s.e.m.

first 3 d; this effect was reduced in knockout mice (Fig. 2e). The early-phase mechanical allodynia was also reduced in knockout mice (Fig. 2f). However, the neuropathic pain symptoms fully developed on day 10 in knockout mice (Fig. 2e,f). Taken together, our data strongly suggest a critical role of MMP-9 in the early development of neuropathic pain. Notably, our MMP-9 knockout mice are not inducible mutants, so compensatory adaptations (for example, MMP-2 upregulation; see below) may have occurred during development. Besides neuropathic pain, inflammatory pain was also reduced in MMP-9-deficient mice (Supplementary Fig. 2c,d).

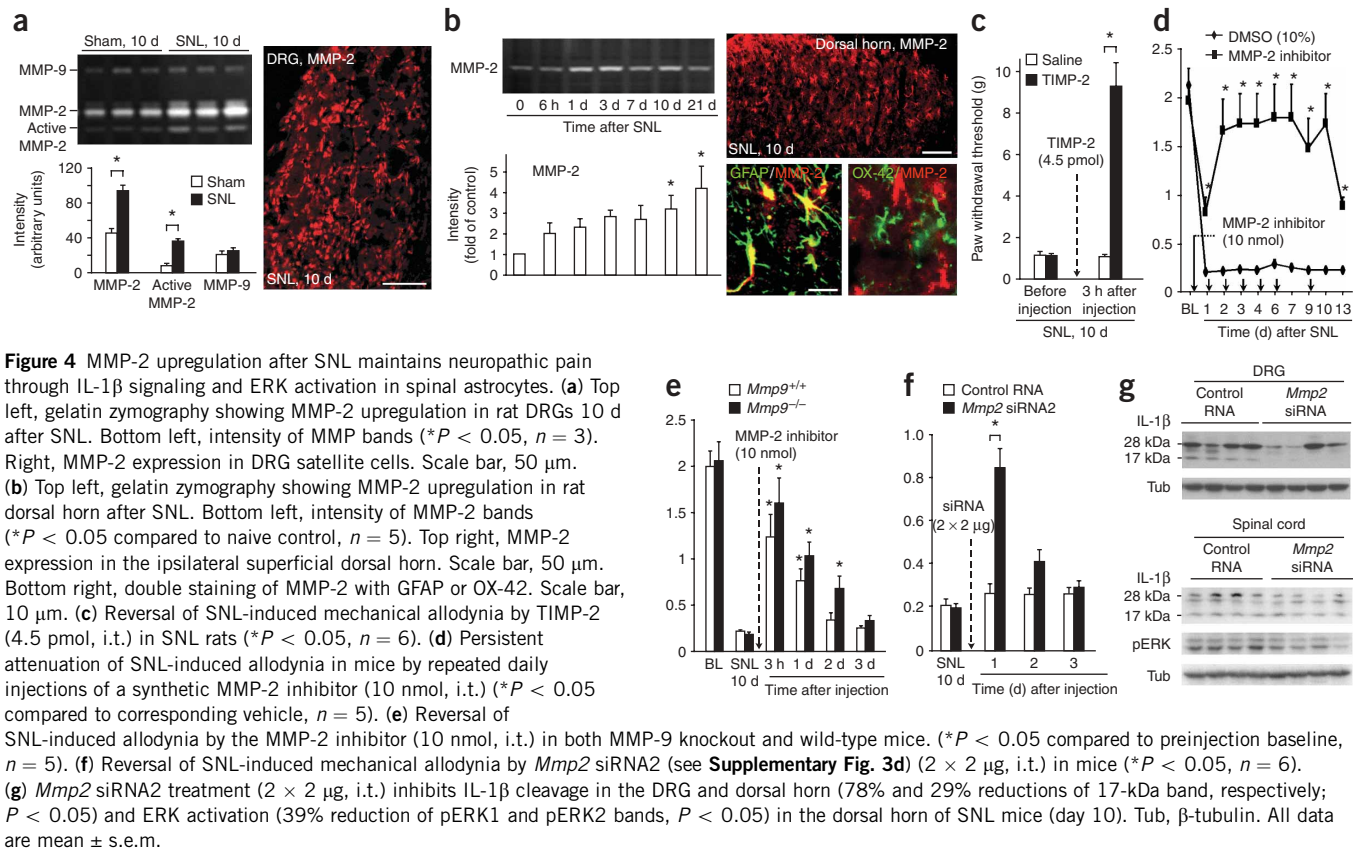
To define the mechanism by which MMP-9 induces neuropathic pain, we examined microglial activation in the spinal cord, an event essential for the pathogenesis of neuropathic pain<sup>15-18</sup>. Intrathecal MMP-9 injection evoked marked microglial activation, as indicated by increased expression of the microglial surface marker OX-42 (CD11b) (Fig. 3a). Because we have previously shown that SNL activates p38 mitogen-activated protein kinase (MAPK) in spinal microglia<sup>19</sup>, we asked whether this pathway could be triggered by exogenous MMP-9. After MMP-9 injection, phosphorylated p38 (P-p38) was exclusively elevated in OX-42<sup>+</sup> microglia (Fig. 3b). Further, spinal microglial and p38 activation after SNL was inhibited by *Mmp9* siRNA treatment (Fig. 3a,b) and in MMP-9-deficient mice (Supplementary Fig. 4 online). Notably, allodynia after MMP-9 and SNL was reversed by a p38 inhibitor (Fig. 3c). Thus, in nerve injury-induced allodynia, p38 activation in spinal microglia may be downstream of MMP-9.

A critical substrate of MMP-9 could be IL-1 $\beta$ <sup>5,20</sup>, which is essential for chronic pain generation<sup>18,21,22</sup>. MMP-9 treatment increased the

cleaved forms of IL-1 $\beta$  in the DRG (Fig. 3d). ELISA analysis, which mainly detects cleaved IL-1 $\beta$ , also showed an IL-1 $\beta$  increase after MMP-9 treatment (Fig. 3e, Supplementary Discussion online). Conversely, SNL-induced IL-1 $\beta$  cleavage was reduced in MMP-9 null mice (Fig. 3d) or after *Mmp9* siRNA treatment (Fig. 3e). IL-1 $\beta$  was expressed in DRG neurons and some satellite cells. Further, IL-1 $\beta$  colocalized with MMP-9 in DRG neurons (Supplementary Fig. 5a online). Notably, inhibiting IL-1 $\beta$  signaling with a neutralizing antibody blocked allodynia triggered by both MMP-9 and SNL (Fig. 3f). Collectively, these data suggest that, in nerve injury-evoked pain, IL-1 $\beta$  may also be downstream of MMP-9.

As a comparison, we also examined the role of caspase-1, a well-known IL-1 $\beta$ -converting enzyme, in the SNL model. Unlike MMP-9, caspase-1 was expressed in DRG satellite cells and was not upregulated after SNL (Supplementary Fig. 5a,b). Intrathecal treatment with the caspase-1 inhibitor *N*-acetyl-Tyr-Val-Ala-Asp-chloromethyl ketone (ac-YVAD-CMK) only moderately inhibited SNL-induced IL-1 $\beta$  cleavage in the DRG (Supplementary Fig. 5c,d). In the spinal cord, IL-1 $\beta$  cleavage by SNL was also reduced in MMP-9 null mice and after *Mmp9* siRNA treatment, and intrathecal MMP-9 increased IL-1 $\beta$  levels (Supplementary Fig. 5e). In contrast, inhibition of spinal caspase-1, which showed no upregulation after SNL and which was expressed in some microglial cells, did not inhibit IL-1 $\beta$  cleavage (Supplementary Fig. 5f,g, Supplementary Discussion). Thus MMP-9 and caspase-1 may regulate IL-1 $\beta$  cleavage under different conditions.

MMP-9 produces neuropathic pain symptoms through IL-1 $\beta$  cleavage and microglial p38 activation (Fig. 3g). MMP-9 and IL-1 $\beta$



may also be released from the central terminals of DRG neurons. There are possible positive feedback loops between cytokines and MMP-9 in the DRG and between IL-1 $\beta$  and p38 in the spinal cord. Intrathecal IL-1 $\beta$  induces spinal p38 activation<sup>23</sup>, and p38 activation further induces IL-1 $\beta$  release<sup>24</sup>. How does IL-1 $\beta$  increase pain sensitivity? In the DRG, IL-1 $\beta$  modulates the activity of sodium channels to increase the excitability of nociceptive neurons (**Supplementary Discussion**). In the spinal cord, IL-1 $\beta$  both enhanced excitatory synaptic transmission and reduced inhibitory synaptic transmission in spinal nociceptive neurons (Y.K. and R.-R.J., unpublished data).

As expected, SNL also caused a profound MMP-9 upregulation in the damaged spinal nerve (**Supplementary Fig. 6a** online), which could lead to demyelination by MMP-9 cleavage of myelin basic protein, a process that might be associated with neuropathic pain<sup>6,25</sup>. MMP-9 expression was low in dorsal root containing central axons but increased after SNL (**Supplementary Fig. 6a**). However, electron microscopy showed no sign of demyelination or degeneration in dorsal root axons after either SNL or intrathecal MMP-9 at an allodynia-producing dose (1 pmol; **Supplementary Fig. 6b–e**). Neither did the MMP-9 injection cause apoptosis of dorsal horn neurons (**Supplementary Fig. 6f**). Therefore, MMP-9-induced allodynia and microglial activation do not result from dorsal root degeneration.

Compared to MMP-9, MMP-2 upregulation after SNL showed different spatial and temporal patterns: SNL induced a delayed upregulation of MMP-2 in the DRG and spinal cord (**Figs. 1a** and **4a,b**). Unlike MMP-9, MMP-2 was found in satellite cells in the DRG (**Fig. 4a**). In the spinal cord, MMP-2 was induced in astrocytes, identified by the astrocyte marker glial fibrillary acidic protein (GFAP) (**Fig. 4b**). Intrathecal administration of TIMP-2, an endogenous tissue inhibitor of MMP-2 (ref. 14), at a very low dose (4.5 pmol), reversed

SNL-induced allodynia on day 10 (**Fig. 4c**). To determine whether neuropathic pain could be persistently attenuated by MMP-2 inhibition, we gave repeated injections of a small synthetic inhibitor of MMP-2 (an *N*-arylsulfonyl-*N*-alkoxyaminoacetohydroxamic acid compound; see **Supplementary Discussion**). This treatment partly attenuated allodynia on day 1 but almost completely blocked allodynia in the following ten days. Notably, the antiallodynic effect lasted for 4 d more after a final injection, suggesting a cumulative effect of the inhibitor (**Fig. 4d**). To exclude a role of MMP-9 in late-phase neuropathic pain, we tested the MMP-2 inhibitor in MMP-9 null mice. This inhibitor produced a more profound antiallodynic effect in knockout mice, owing to MMP-2 compensation in these mice (**Fig. 4e**, **Supplementary Fig. 7a** online). SNL-induced allodynia was also reversed by specific MMP-2 knockdown with an siRNA (**Fig. 4f**, **Supplementary Fig. 3d–g**). Conversely, intrathecal infusion of MMP-2 produced allodynia (**Supplementary Fig. 7b**).

How can MMP-2 maintain neuropathic pain? Because MMP-2 was also implicated in IL-1 $\beta$  cleavage<sup>5,20</sup>, we tested this possibility late after SNL. IL-1 $\beta$  cleavage in the DRG and spinal cord at SNL day 10 was inhibited by *Mmp2* siRNA (**Fig. 4g**). Intrathecal MMP-2 consistently enhanced IL-1 $\beta$  cleavage (**Supplementary Fig. 7b**). Allodynia was also reversed by neutralizing IL-1 $\beta$  in both wild-type and MMP-9 null mice (**Supplementary Fig. 7c**).

Recent studies have proposed a role for spinal astrocytes in maintaining neuropathic pain<sup>12</sup>. In particular, the extracellular signal-regulated kinase (ERK) MAP kinase is activated in spinal astrocytes at late times after nerve injury (**Supplementary Fig. 7d**), which is required for persistent allodynia in both rats<sup>26</sup> and mice (data not shown). Administration of *Mmp2* siRNA or TIMP-2 reduced SNL-induced ERK activation in spinal astrocytes, indicating a role

of MMP-2 in ERK activation (Fig. 4g, Supplementary Fig. 7d). Further, in cultured astrocytes, IL-1 $\beta$  treatment activated ERK and released MMP-2 (Supplementary Fig. 7e). MMP-2 upregulation maintains neuropathic pain by IL-1 $\beta$  cleavage and astroglial activation of ERK (Supplementary Fig. 7f). These data suggest a positive feedback loop between IL-1 $\beta$  and MMP-2.

In summary, our findings have revealed new mechanisms of neuropathic pain. First, we have demonstrated different temporal upregulation and cellular localization of MMP-9 and MMP-2. Second, we have shown that MMP-9 produced in injured DRG neurons serves as one of the triggers for spinal microglial activation and neuropathic pain development and that MMP-9-induced pathophysiology involves IL-1 $\beta$  cleavage and microglial p38 activation. Third, we have illustrated that MMP-2 produces late-phase neuropathic pain by IL-1 $\beta$  cleavage and astrocytic ERK activation. Finally, we have shown that endogenous inhibitors of MMP (TIMP-1 and TIMP-2) are powerful agents for suppressing neuropathic pain. Given the critical role of MMP-9 and MMP-2 in early- and late-phase neuropathic pain, MMP-9 inhibition may alleviate some early-phase neuropathic pain conditions induced by major surgeries (for example, thoracotomy during cardiac surgeries) or chemotherapy<sup>3,4,27</sup>, whereas MMP-2 inhibition may attenuate established neuropathic pain conditions (for example, diabetic neuropathy). Ideally, dual inhibition of MMP-2 and MMP-9 may alleviate neuropathic pain at different phases. However, the network responses of other MMPs and their roles in neuropathic pain remain to be assessed.

## METHODS

**Animals and surgery.** We purchased male adult Sprague-Dawley rats (200–260 g) from Charles River Laboratories and obtained male MMP-9 null (*Mmp9*<sup>-/-</sup>) mice and FVB control wild-type mice (25–35 g) from Jackson Laboratories. The knockout mice are fertile and do not show differences in overall weight and behavior compared with wild-type mice. MMP-9 null mice were backcrossed to the FVB background for more than five generations. The Harvard Medical School Animal Care Committee approved all animal procedures in this study. We anesthetized animals with sodium pentobarbital (50 mg/kg) or isoflurane. To produce a spinal nerve ligation, we removed the transverse process of the L5 lumbar vertebra to expose the L4 and L5 spinal nerves. The L5 spinal nerve was then isolated and tightly ligated with 6-0 silk thread. We used sham surgery (exposure of the spinal nerves without ligation) as a control. To produce inflammatory pain, we injected carrageenan (2%, 20  $\mu$ l) into a mouse hindpaw. See **Supplementary Methods** online for more details.

**Drugs and administration.** We purchased MMP-9 inhibitor (Inhibitor-I), MMP-2 inhibitor (Inhibitor-III) and caspase-1 inhibitor II, *N*-acetyl-Tyr-Val-Ala-Asp-chloromethyl ketone (ac-YVAD-CMK) from Calbiochem; MMP-9, TIMP-1 and TIMP-2 from Chemicon; MMP-2, IL-1 $\beta$  and IL-1 $\beta$ -neutralizing antibody from R&D Systems; and thalidomide (TNF- $\alpha$ -synthesis inhibitor) from Sigma. The p38 inhibitor FR167653 was kindly provided by T. Kohno (Niigata University). The drug doses were selected on the basis of previous reports and our preliminary studies. siRNAs targeting *Mmp9* and *Mmp2* and mismatch control siRNAs (21 base pairs) were synthesized by Dharmacon. To deliver siRNA into cells, we used polyethyleneimine, a cationic polymer, as a delivery vehicle to prevent degradation and enhance cell membrane penetration of siRNAs<sup>28</sup>. The drugs or their vehicles (DMSO, saline or normal serum) were delivered intrathecally into cerebral spinal fluid through lumbar puncture or with an osmotic pump through an intrathecally implanted catheter. The MMP-9 inhibitor was infused by an osmotic pump for 7 d at 0.5  $\mu$ l (0.2  $\mu$ g) per hour, starting 2 d before SNL. See **Supplementary Methods** for more details.

**Gelatin zymography.** We anesthetized animals deeply with isoflurane and transcardially perfused them with PBS. We then rapidly dissected L5 DRGs, spinal nerves, dorsal roots and spinal dorsal horn segments and homogenized

them in SDS lysis buffer containing proteinase inhibitors. We loaded 10  $\mu$ g of protein per lane into the wells of precast gels (10% polyacrylamide minigels containing 0.1% gelatin, Novex). After electrophoresis, each gel was incubated with 100 ml of development buffer<sup>8</sup>. Commercial MMP-9 and MMP-2 were used as standards. See **Supplementary Methods** for more details.

**Western blotting.** We perfused animals transcardially with PBS after deep anesthesia with isoflurane. We then rapidly removed the DRGs, spinal nerves, dorsal roots and spinal cord segments and homogenized them in a lysis buffer containing a cocktail of proteinase inhibitors and phosphatase inhibitors. The protein concentrations were determined by BCA Protein Assay (Pierce), and 30  $\mu$ g of proteins were loaded and separated on SDS-PAGE gels (4–15%, Bio-Rad). After transfer, blots were incubated overnight at 4 °C with polyclonal antibody to MMP-9 (1:1,000, Chemicon), MMP-2 (1:1,000, Torrey Pines), IL-1 $\beta$  (1:1,000, Chemicon), caspase-1 (1:500, Abcam) or phosphorylated ERK (1:1,000, Cell Signaling). For loading control, the blots were probed with  $\beta$ -tubulin or ERK2 antibody.

**Immunohistochemistry.** We anesthetized animals deeply with isoflurane and perfused through the ascending aorta with saline followed by 4% paraformaldehyde. We then excised DRG and spinal cord tissues and postfixed them in this fixative overnight. Tissue sections were cut in a cryostat and processed for immunofluorescence. All sections were blocked with 2% goat serum and incubated overnight at 4 °C with primary antibody, followed by Cy3- or FITC-conjugated secondary antibody. For double immunofluorescence, sections were incubated with a mixture of polyclonal and monoclonal primary antibodies followed by a mixture of FITC- and Cy3-conjugated secondary antibodies. We tested the specificity of immunostaining and antibodies by (i) omission of the primary antibody and (ii) absorption of antibodies with respective peptide antigens. See more details in **Supplementary Methods**.

**Electron microscopy.** We collected L5 dorsal roots close to the L5 DRGs and fixed them in 4% paraformaldehyde and 2.5% glutaraldehyde for 48 h at 4 °C, then washed in PBS, osmicated, dehydrated and embedded in epoxy. Ultrathin sections were cut, collected on cellulose-coated single-slot grids, stained with uranyl acetate and lead citrate, and photographed with a Jeol 1200EX electron microscope<sup>29</sup>.

**ELISA.** We purchased a rat IL-1 $\beta$  ELISA kit from R&D Systems and performed the ELISA according to the manufacturer's protocol, using 100  $\mu$ g protein. We included the standard curve in each experiment.

**Primary DRG culture.** We aseptically removed DRGs from 2- to 3-week-old rats and digested the tissues with collagenase (1.25 mg/ml) and dispase-II (2.4 units/ml) for 90 min, followed by 0.25% trypsin for 8 min at 37 °C. We plated cells on slide chambers coated with poly-D-lysine and laminin or plates coated with poly-D-lysine and grew them in a neurobasal defined medium (Gibco) for 24 h before experiments. See **Supplementary Methods** for more details.

**Primary astrocyte culture.** We prepared astroglial cultures from cerebral cortices of neonatal rats. The meninges were removed from cortices in Hanks buffer. We plated cells at  $2.5 \times 10^5$ /ml in a medium containing 15% FBS in low-glucose DMEM and maintained them for 3 weeks. The medium was replaced twice weekly, first with 15% FBS, then with 10% FBS and finally with 10% horse serum.

**Behavioral analysis.** Animals were habituated to the testing environment daily for at least 2 d before baseline testing. For testing mechanical sensitivity, we placed animals in boxes on an elevated metal mesh floor and allowed them 30 min for habituation before examination. We stimulated the plantar surface of each hindpaw with a series of von Frey hairs with logarithmically incrementing stiffness (Stoelting), presented perpendicular to the plantar surface. The 50% paw withdrawal threshold was determined using Dixon's up-down method. To measure spontaneous pain in mice, we counted the number of paw flinches over a 2-min period and averaged the numbers after three trials.

**Quantification and statistics.** We measured the density of specific MMP bands from gelatin zymography and western blotting and the density of

immunoreactive DRG neurons with a computer-assisted imaging analysis system. We counted the number of immunoreactive cells in the medial superficial laminae (I–III) of the spinal cord (see more details in **Supplementary Methods**). Data are expressed as mean  $\pm$  s.e.m. Differences between groups were compared using Student's *t*-test or analysis of variance. The criterion for statistical significance was  $P < 0.05$ .

*Note: Supplementary information is available on the Nature Medicine website.*

#### ACKNOWLEDGMENTS

The work was supported in part by US National Institutes of Health grants R01-DE17794, R01-NS54362 and TW7180 to R.-R.J. and R01-NS37074, R01-NS48422, R01-NS56458, P01-NS55104 and P50-NS10828 to E.H.L. P.-H.T. was supported by a grant from E-DA Hospital/I-Shou University, Taiwan. We thank T. Kohno (Niigata University, Japan) for providing FR167653 compound and Q. Ma (Harvard Medical School) for critical reading of the manuscript.

#### AUTHOR CONTRIBUTIONS

Y.K. performed behavioral and immunohistochemical experiments; Z.-Z.X. conducted western blotting, DRG culture and zymography studies; X.W. performed zymography studies and contributed to project development; J.Y.P. conducted behavioral studies; Z.-Y.Z. conducted initial behavioral and histochemical studies; P.-H.T. designed siRNAs and initially tested MMP-9 siRNA; Y.-J.G. conducted ELISA studies and prepared astrocyte cultures; K.R. and G.C. contributed to electron microscopy studies; E.H.L. developed the project and provided critical review and comments on the manuscript. R.-R.J. developed and supervised the project, designed all the experiments, conducted some data analysis and prepared the manuscript.

Published online at <http://www.nature.com/naturemedicine>

Reprints and permissions information is available online at <http://npg.nature.com/reprintsandpermissions>

- Ji, R.R. & Strichartz, G. Cell signaling and the genesis of neuropathic pain. *Sci. STKE* **2004**, reE14 (2004).
- Tsuda, M., Inoue, K. & Salter, M.W. Neuropathic pain and spinal microglia: a big problem from molecules in "small" glia. *Trends Neurosci.* **28**, 101–107 (2005).
- Woolf, C.J. & Mannion, R.J. Neuropathic pain: aetiology, symptoms, mechanisms, and management. *Lancet* **353**, 1959–1964 (1999).
- Kehlet, H., Jensen, T.S. & Woolf, C.J. Persistent postsurgical pain: risk factors and prevention. *Lancet* **367**, 1618–1625 (2006).
- Parks, W.C., Wilson, C.L. & Lopez-Boado, Y.S. Matrix metalloproteinases as modulators of inflammation and innate immunity. *Nat. Rev. Immunol.* **4**, 617–629 (2004).
- Chattopadhyay, S., Myers, R.R., Janes, J. & Shubayev, V. Cytokine regulation of MMP-9 in peripheral glia: Implications for pathological processes and pain in injured nerve. *Brain Behav. Immun.* **21**, 561–568 (2007).
- Rosenberg, G.A. Matrix metalloproteinases in neuroinflammation. *Glia* **39**, 279–291 (2002).
- Wang, X. *et al.* Effects of matrix metalloproteinase-9 gene knock-out on morphological and motor outcomes after traumatic brain injury. *J. Neurosci.* **20**, 7037–7042 (2000).
- Yong, V.W. Metalloproteinases: mediators of pathology and regeneration in the CNS. *Nat. Rev. Neurosci.* **6**, 931–944 (2005).
- Zhao, B.Q. *et al.* Role of matrix metalloproteinases in delayed cortical responses after stroke. *Nat. Med.* **12**, 441–445 (2006).
- Kim, S.H. & Chung, J.M. An experimental model for peripheral neuropathy produced by segmental spinal nerve ligation in the rat. *Pain* **50**, 355–363 (1992).
- Zhuang, Z.Y. *et al.* A peptide c-Jun N-terminal kinase (JNK) inhibitor blocks mechanical allodynia after spinal nerve ligation: respective roles of JNK activation in primary sensory neurons and spinal astrocytes for neuropathic pain development and maintenance. *J. Neurosci.* **26**, 3551–3560 (2006).
- Levin, J.I. *et al.* The discovery of anthranilic acid-based MMP inhibitors. Part 3: incorporation of basic amines. *Bioorg. Med. Chem. Lett.* **11**, 2975–2978 (2001).
- Murphy, G. & Willenbrock, F. Tissue inhibitors of matrix metalloproteinases. *Methods Enzymol.* **248**, 496–510 (1995).
- Coull, J.A. *et al.* BDNF from microglia causes the shift in neuronal anion gradient underlying neuropathic pain. *Nature* **438**, 1017–1021 (2005).
- Raghavendra, V., Tanga, F. & DeLeo, J.A. Inhibition of microglial activation attenuates the development but not existing hypersensitivity in a rat model of neuropathy. *J. Pharmacol. Exp. Ther.* **306**, 624–630 (2003).
- Tsuda, M. *et al.* P2X4 receptors induced in spinal microglia gate tactile allodynia after nerve injury. *Nature* **424**, 778–783 (2003).
- Watkins, L.R., Milligan, E.D. & Maier, S.F. Glial activation: a driving force for pathological pain. *Trends Neurosci.* **24**, 450–455 (2001).
- Jin, S.X., Zhuang, Z.Y., Woolf, C.J. & Ji, R.R. p38 mitogen-activated protein kinase is activated after a spinal nerve ligation in spinal cord microglia and dorsal root ganglion neurons and contributes to the generation of neuropathic pain. *J. Neurosci.* **23**, 4017–4022 (2003).
- Schonbeck, U., Mach, F. & Libby, P. Generation of biologically active IL-1 $\beta$  by matrix metalloproteinases: a novel caspase-1-independent pathway of IL-1 $\beta$  processing. *J. Immunol.* **161**, 3340–3346 (1998).
- Samad, T.A. *et al.* Interleukin-1 $\beta$ -mediated induction of Cox-2 in the CNS contributes to inflammatory pain hypersensitivity. *Nature* **410**, 471–475 (2001).
- Sweitzer, S., Martin, D. & DeLeo, J.A. Intrathecal interleukin-1 receptor antagonist in combination with soluble tumor necrosis factor receptor exhibits an anti-allodynic action in a rat model of neuropathic pain. *Neuroscience* **103**, 529–539 (2001).
- Sung, C.-S. *et al.* Inhibition of p38 mitogen-activated protein kinase attenuates interleukin-1 $\beta$ -induced thermal hyperalgesia and inducible nitric oxide synthase expression in the spinal cord. *J. Neurochem.* **94**, 742–752 (2005).
- Clark, A.K. *et al.* Rapid co-release of interleukin 1 $\beta$  and caspase 1 in spinal cord inflammation. *J. Neurochem.* **99**, 868–880 (2006).
- Inoue, M. *et al.* Initiation of neuropathic pain requires lysophosphatidic acid receptor signaling. *Nat. Med.* **10**, 712–718 (2004).
- Zhuang, Z.Y., Gerner, P., Woolf, C.J. & Ji, R.R. ERK is sequentially activated in neurons, microglia, and astrocytes by spinal nerve ligation and contributes to mechanical allodynia in this neuropathic pain model. *Pain* **114**, 149–159 (2005).
- Dworkin, R.H. *et al.* Advances in neuropathic pain: diagnosis, mechanisms, and treatment recommendations. *Arch. Neurol.* **60**, 1524–1534 (2003).
- Tan, P.H., Yang, L.C., Shih, H.C., Lan, K.C. & Cheng, J.T. Gene knockdown with intrathecal siRNA of NMDA receptor NR2B subunit reduces formalin-induced nociception in the rat. *Gene Ther.* **12**, 59–66 (2005).
- Chen, S. *et al.* Disruption of ErbB receptor signaling in adult non-myelinating Schwann cells causes progressive sensory loss. *Nat. Neurosci.* **6**, 1186–1193 (2003).